Broadband Measurement of Error Vector Magnitude for Microwave Vector Signal Generators Using a Vector Network Analyzer

Alberto Maria Angelotti, *Member, IEEE*, Gian Piero Gibiino, *Member, IEEE*, Alberto Santarelli, *Member, IEEE*, and Pier Andrea Traverso, *Member, IEEE*

***Abstract*— A frequency-domain method is proposed for the broadband measurement of error vector magnitude (EVM) for vector signal generators (VSGs). The technique is based on frequency-swept narrowband acquisitions performed with a vector network analyzer (VNA) by exploiting a stable (yet unknown) reference signal to obtain phase-repeatable measurements, eventually allowing to refer the residual distortion contribution of the analog VSG output to its digital input. The method leverages on the formulation of a novel measurement-based model, which accounts for the IQ imbalance effect and allows to separate it from the actual distortion within the VSG, ultimately yielding accurate broadband EVM measurements at microwave carrier frequencies without any time-domain waveform reconstruction, completely avoiding the use of broadband receivers and corresponding calibration.**

***Index Terms*— Error vector magnitude (EVM), in-phase/quadrature (IQ) modulators, modulation distortion, vector signal generators (VSGs).**

I. Introduction

NOVEL communication standards featuring ever broader bandwidths (BWs) are currently being adopted in order to satisfy the increasing need for higher data rates. For example, the fifth generation of mobile telecommunications (5G) implements orthogonal frequency-division multiplexing (OFDM) modulation schemes with BWs of up to 400 MHz per channel for Frequency Range 2 (FR2) at carrier frequencies in the lower millimeter-wave bands [1]. Since modulations like high-order OFDM can effectively be employed only when sufficient signal quality is achieved across the whole transmitter/receiver chain, it is crucial to characterize equipment with metrics [2] that can properly describe the actual broadband performance of the components in use. In this sense, the most critical devices within the transmission stage of radio frequency (RF) systems are the nonlinear ones, such as power amplifiers (PAs) and frequency converters.

Experimental approaches for characterizing the nonlinear distortion of a microwave device-under-test (DUT) are often based on continuous-wave (CW) single- or two-tone excitations [3], [4] yielding classical linearity metrics such as gain compression and intermodulation distortion (IMD). However, these techniques poorly reproduce the actual linearity performance of systems operating under modulated excitation. The error vector magnitude (EVM) [5] is instead preferred as a relevant metric to quantify broadband distortion.

In a standard EVM characterization setup, the input of the DUT is excited using a vector signal generator (VSG), whereas the output signal is measured by a vector signal analyzer (VSA). The input consists of a suitable applicationlike signal, i.e., complex test signals featuring in-phase/quadrature (IQ) modulation. The output signal contains, in general, the combined distortion and nonlinear impairments by both the VSG and the DUT. After performing an equalization to compensate for the linear response of the test set, the output signal is finally demodulated into its I and Q components. Given an ideal reference constellation, the EVM estimate can be mathematically computed from the time-domain envelope waveforms as the ratio of the power of the deviation from the ideal constellation to the total received power. Since this standard procedure requires coherent IQ demodulation, the VSA front-end must feature a wider instantaneous BW than the one occupied by the input test signal. This constraint is particularly challenging for broadband signals at microwave frequencies (e.g., FR2), as suitable hardware for demodulation and digitization can be extremely costly and/or feature a reduced dynamic range.

In order to overcome this limitation, a variety of methods has been proposed [6]–[8]. Instead of a VSA, these approaches make use of the acquisition receivers available in vector network analyzers (VNAs) [9], [10] to perform EVM measurements across wider BWs, possibly extending to the whole frequency range of the VNA test-set (i.e., several gigahertz), with a high degree of accuracy. These methods are based on multiple measurements of the response to multitone periodic input signals specifically designed to display the same statistical properties as standard-compliant OFDM test signals [7], [8], [11], [12]. Such a configuration is depicted in Fig. 1(a), showing the particular case of a PA as a DUT.

A VNA performs measurements in a frequency-swept fashion, where the spectral components are demodulated with a sweeping local oscillator (LO) frequency (f_{LO}) to the intermediate frequency (IF) at f_{IF}, then digitized by the internal

Manuscript received 1 February 2022; revised 14 May 2022; accepted 30 May 2022. Date of publication 9 June 2022; date of current version 22 June 2022. The Associate Editor coordinating the review process was Zhengyu Peng. *(Corresponding author: Alberto Maria Angelotti.)*

The authors are with the Department of Electrical, Electronic, and Information Engineering "Guglielmo Marconi," University of Bologna, 40136 Bologna, Italy (e-mail: alberto.angelotti@unibo.it).

Digital Object Identifier 10.1109/TIM.2022.3181904

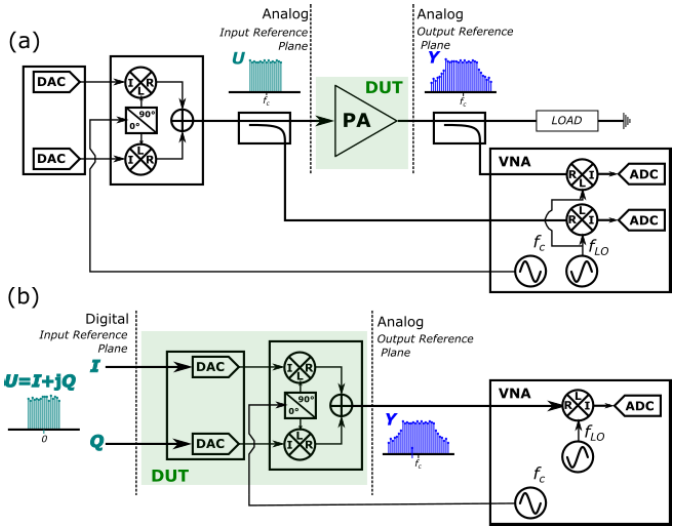

Fig. 1. (a) Block diagram of a VNA-based EVM characterization setup for a two-port RF PA where U is the analog RF input. (b) Block diagram of a VNA-based EVM characterization setup for a VSG including IQ modulation, where $U = I + jQ$ is the digital BB input.

analog-to-digital converters (ADCs). Classical VNA measurements prevent the reconstruction of time-domain demodulated waveforms, given that the frequency components are measured in separate acquisitions and that each acquisition involves an unknown and different LO phase. As only calibrated ratios between acquisitions at different receivers are available, this configuration does not allow to estimate the EVM value by directly comparing the constellation measured at the output of the DUT versus the reference one.

Nevertheless, it has been shown [7], [13] that the residual EVM contribution by the DUT only (separated from the one by the VSG) can be accurately estimated with a VNA through spectral correlations between the measured waveforms at the input (incident traveling wave on the first port) and output (reflected traveling wave on the second port) of the DUT. More in detail, the EVM measurement process can be designed so as to make solely use of ratios between the two measured waveforms, with the superimposed unknown LO phase profile across frequency getting canceled out within the procedure. This type of VNA-based solutions has been shown to be extremely valuable in providing accurate EVM estimates, making efficient use of existing hardware, and leveraging on both the typical high dynamic range of VNA narrowband receivers and the broadband frequency characteristics of the microwave test-set (i.e., directional couplers and mixers). Moreover, the availability of multiple receivers in VNA architectures has been used to flexibly perform EVM measurements in other scenarios, e.g., in combination with load-pull for PAs [10].

Given these advantages, it is interesting to consider VNA-based methods also for IQ modulators [14], [15] and VSGs. While a procedure has been proposed for the case of a passive IQ mixer [15], where the traveling waves at both input (at IF) and output (at RF) are accessible for measurement, the application to VSGs (i.e., to modulated sources) is not straightforward, as they embed digital-to-analog (D/A) conversion, IF synthesis, and IQ modulation, without the possibility of signal probing in between these stages [see Fig. 1(b)]. Indeed, only the output signal is available as an analog quantity at the output of the DUT, whereas the input corresponds to the complex baseband (BB) envelope at a numerical reference plane before D/A conversion. As a consequence, a proper EVM measurement procedure for VSGs should ideally quantify the distortion with respect to the ideal modulated signal loaded into the VSG digital memory. However, the absence of a measurable analog input at the same frequency as the output prevents, in principle, from removing the random phase contribution due to the LO.

This work presents a novel VNA-based approach for the characterization of modulation distortion metrics (in particular, EVM) applicable to VSGs, i.e., IQ-modulated sources featuring a digital BB interface. The proposed method leverages on the use of an additional reference signal measured on a second VNA channel. This auxiliary channel allows to compensate for the random LO phase shifts introduced by the VNA receiver on the output of the VSG (i.e., the DUT), so as to obtain phase-repeatable [16] acquisitions.

Since no *a priori* knowledge of the reference signal characteristics (and in particular, its phase spectrum) is used, the proposed approach fundamentally differs from those based on the reconstruction of time-domain waveforms, as well as from the ones assuming either a known (or precharacterized) phase reference [16]–[18] or a precalibrated reference receiver. As a consequence, the proposed technique completely avoids the implementation of waveform traceability to fundamental metrological standards, which is generally a complex and costly process [2], particularly for the tight spectral grids required by EVM test signals at microwave carrier frequencies [19]. The technique is also different from phase-stitching methods [20], in which each given frequency component of an unknown reference signal is measured multiple times using different LO frequencies to deembed the reciprocal phase variations and reconstruct the time-domain signal. In fact, the proposed technique does not extract at all the actual phase-coherent time-domain waveform at the output of the DUT. Yet, the available information is nevertheless shown to be sufficient for computing the EVM.

In addition, the proposed characterization procedure makes use of a novel measurement model based on the best-linear-approximation (BLA) theory, which is specifically tailored to the quantification of modulation distortion introduced by the IQ modulator. Differently from general system theory approaches [21], this model specifically considers the large-signal IQ imbalance in the two modulator branches, so as to allow for a more accurate estimation of the EVM.

The work is organized as follows. Section II presents the BLA framework for EVM estimation, and it extends its validity to the specific case of VSG with IQ imbalance. Section III outlines the concept of phase-repeatable acquisitions with a VNA using a reference channel, then describes the BLA framework to VSGs under test with a digital input interface. Section IV shows the VNA-based measurement setup, whereas the experimental results validating the methods are reported in Section V. Finally, conclusions are drawn in Section VI.

II. Best Linear Approximation Framework for Measuring the EVM of a VSG

A. Best Linear Approximation Theory

The VNA-based approaches proposed in literature for measuring EVM [7]–[9] leverage on the BLA framework [21] applied to the nonlinear DUT. As commonly assumed in these implementations, all the signals under consideration are periodic, thus feature a discrete spectrum on a regularly-spaced frequency grid. Hence, a frequency domain description will be used in the following. From the BLA theory, it can be shown that the output of any single-input single-output (SISO) nonlinear-dynamic periodic-input-same-period-output (PISPO) system can be decomposed as [see Fig. 2(a)]

$$Y(f) = H(f)U(f) + D_Y(f) \tag{1}$$

where U and Y are the input and the output of the system, respectively, at the generic frequency f. The term H, also known as the BLA gain, is the frequency response function (FRF) of the equivalent linear time-invariant (LTI) system that best approximates the behavior of the actual system (in the mean-least-square sense) for a given excitation signal class. As the system (i.e., the DUT) is nonlinear, an LTI approximation is not sufficient to capture its complete behavior. In (1), the residual nonlinear contribution is embodied by D_Y, which takes the name of nonlinear stochastic distortion, since it can be shown to behave as a noiselike source with zero average ($\mathbb{E}[D_Y] = 0$, $\mathbb{E}[\cdot]$ being the statistical expectation) uncorrelated with the input ($\mathbb{E}[D_Y U^*] = 0$). At the same time, D_Y is clearly not independent of the input signal U, as it expresses the nonlinear distortion components originated by it.

Due to the uncorrelation property, the BLA gain of a PISPO system can be found as

$$H(f) = \frac{\mathbb{E}\big[Y(f)U(f)^*\big]}{\mathbb{E}\big[U(f)U(f)^*\big]} = \frac{S_{YU}(f)}{S_{UU}(f)} \tag{2}$$

where S_{UU} and S_{YU} correspond to the self and cross bilateral power spectral densities (PSDs), respectively.

Considering a large-signal operating point (LSOP) for the DUT, this description is applicable to waveforms originated from a stationary stochastic process with a given probability density function (pdf) and PSD. The typical application case is to consider signals belonging to the complex-Gaussian class with a band-limited PSD [21], which includes band-limited Gaussian noise, random-phase multitones, and OFDM waveforms with a sufficiently large number of subcarriers [8]. More in general, it is possible to design multitone waveforms to closely approximate the spectral and statistical properties [12], [22] of any communication standard of interest. In this work, the excitation signals will consist of random-phase multitones with constant band-limited PSD, which feature particularly favorable properties [21] yet still providing a good approximation to Gaussian OFDM waveforms used in applications, e.g., mobile telecommunication standards [1].

From a practical perspective, the statistical expectation operator $\mathbb{E}[\cdot]$ in (2) is approximately computed by suitably averaging the results across multiple experiments that constitute different realizations of the underlying stochastic process [21]. The DUT is excited using $L \geq 2$ different phase-realizations $U_1, \ldots, U_L$ of flat-amplitude multitone signals and collecting the responses $Y_1, \ldots, Y_L$. In particular, at each frequency f, the following matrices can be defined:

$$\mathbf{Y}(f) = \begin{bmatrix} Y_1(f) \\ \vdots \\ Y_L(f) \end{bmatrix}, \quad \mathbf{U}(f) = \begin{bmatrix} U_1(f) \\ \vdots \\ U_L(f) \end{bmatrix}. \tag{3}$$

The BLA at each frequency f is found by the following pseudo-inverse matrix calculation:

$$H(f) = \big(\mathbf{U}^\dagger(f)\mathbf{U}(f)\big)^{-1}\mathbf{U}^\dagger(f)\mathbf{Y}(f) \tag{4}$$

where $\dagger$ denotes the Hermitian-transpose operator. Once the BLA is known, the PSD of D_Y can be found as

$$\begin{aligned} S_{D_Y D_Y}(f) &= \mathbb{E}\big[|D_Y(f)|^2\big] \\ &= \mathbb{E}\big[|Y(f)|^2\big] - |H(f)|^2\mathbb{E}\big[|U(f)|^2\big] \\ &= S_{YY}(f) - |H(f)|^2 S_{UU}(f) \end{aligned} \tag{5}$$

where S_{UU} and S_{YY} are the input and output signal PSDs, respectively. Just as done for obtaining H, it is possible to find approximations for the expected values by averaging measurements of the input and output power spectra. Finally, the EVM

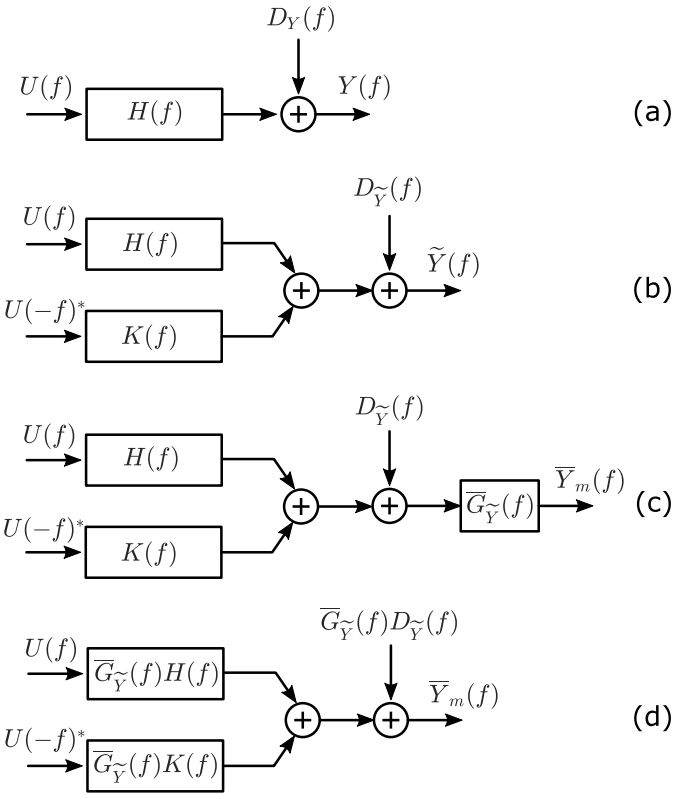

Fig. 2. Block diagram representation of the measurement-based EVM model for different configurations. (a) Classical SISO device. (b) IQ modulator in the envelope domain with separate IQ imbalance term K. (c) IQ modulator in the envelope domain as in (b) cascaded with LTI function $\overline{G}_{\widetilde{Y}}$ due to VNA acquisition process embedding the random yet phase-repeatable contribution due to the LO and triggering. (d) IQ modulator in the envelope domain equivalent to (c) with new distortion term $\overline{G}_{\widetilde{Y}}(f)D_{\widetilde{Y}}(f) = \overline{D}_{\widetilde{Y}}(f)$ and new BLA terms $\overline{G}_{\widetilde{Y}}(f)H(f) = \overline{H}(f)$ and $\overline{G}_{\widetilde{Y}}(f)K(f) = \overline{K}(f)$.

can be computed by integrating the correlated and uncorrelated signal PSDs across the input-excited BW of interest [7]

$$\mathrm{EVM} = \sqrt{\frac{\int_{\mathrm{BW}} S_{D_Y D_Y}(f)df}{\int_{\mathrm{BW}} S_{YY}(f)df}}. \tag{6}$$

Equation (5) shows that the PSD of the nonlinear stochastic distortion is defined in terms of a deviation from the term $|H(f)|^2 S_{UU}(f)$, i.e., a deviation from the part of the output signal correlated with the input through the BLA. This means that LTI effects in the frequency response of the DUT are not included in the EVM. Indeed, like in classical VSA-based systems, the EVM definition in (6) correctly quantifies only the purely nonlinear distortion that cannot be compensated by linear equalization.

B. Best Linear Approximation for an IQ Vector Generator

In order to apply the VNA-based BLA framework to the case of a VSG [which inherently involves frequency conversion, as can be seen in Fig. 1(b)], the input of the system can be indicated with the complex BB signal $U(f) = I(f) + jQ(f)$, where I and Q are the IQ real signals uploaded onto the digital-to-analog converters (DACs) of the VSG. Without loss of generality, the output of the system can be similarly defined as the BB-equivalent (i.e., low-pass complex envelope) representation $\widetilde{Y}$ for a given carrier frequency f_c of the RF signal Y at the output of the VSG, so that

$$Y(f) = \frac{\widetilde{Y}(f - f_c) + \widetilde{Y}(-f - f_c)^*}{2} \tag{7}$$

is satisfied. This choice eventually results in an iso-frequency input–output formulation.

While in (1) the output of a nonlinear dynamic DUT was described in terms of the output of a single, best representative linear system (the BLA), the linear behavior of IQ modulators is typically treated in literature by adding a separate term to explicitly account for the effects of imbalance between the IQ paths. In frequency domain, this nonideality induces a dependence of the output on the conjugate frequency-reverse of the input, i.e., $U(-f)^*$ [14].

In this light, as depicted in Fig. 2(b), the following complex envelope formulation for the nonlinear dynamic behavior of IQ upconverters is proposed:

$$\widetilde{Y}(f) = H(f)U(f) + K(f)U(-f)^* + D_{\widetilde{Y}}(f) \tag{8}$$

where the term H represents the BLA referred to the complex input U, whereas the IQ imbalance term K, similar to H, plays the role of a *best* estimated IQ imbalance component in the given LSOP and for the excitation signal class of interest.

By addressing the IQ imbalance with the separate term K, dedicated IQ linear calibration procedures can be applied [14], [23]. Indeed, just like the component linearly correlated with the input (H) is normally equalized out at the receiver for EVM calculation, K can also be compensated for through measurement-based equalization procedures, hence removing its effects from the distortion contribution. Thus, the nonlinear stochastic distortion $D_{\widetilde{Y}}(f)$ in (8) can be eventually defined as the part of the output $\widetilde{Y}(f)$ that is uncorrelated both with the input $U(f)$ and its conjugate-frequency reversed version $U(-f)^*$. This closely resembles the decomposition adopted for general multiple-input multiple-output (MIMO) nonlinear dynamic systems [24], in which the stochastic distortion term of each output is assumed to be uncorrelated with all inputs. In this respect, the IQ modulator can be effectively treated as a two-input nonlinear system, with the two inputs being the input signal and its conjugate symmetric version.

With the additional assumption that the excitations of interest can be chosen so that $\mathbb{E}[U(f)U(-f)] = 0$, which is valid for random phase multitones, and whose general implications are discussed in the Appendix, the two BLA terms in (8) can be found as

$$\begin{aligned} H(f) &= \frac{\mathbb{E}\left[\tilde{Y}(f)U(f)^*\right]}{\mathbb{E}\left[U(f)U(f)^*\right]} = \frac{S_{\tilde{Y}U}(f)}{S_{UU}(f)} \\ K(f) &= \frac{\mathbb{E}\left[\tilde{Y}(f)U(-f)\right]}{\mathbb{E}\left[U(-f)U(-f)^*\right]} = \frac{\mathbb{E}\left[\tilde{Y}(f)U(-f)\right]}{S_{UU}(-f)} \end{aligned} \tag{9}$$

while the PSD of the nonlinear stochastic distortion term corresponds to

$$\begin{aligned} S_{D_{\tilde{Y}} D_{\tilde{Y}}}(f) &= \mathbb{E}\left[|D_{\tilde{Y}}(f)|^2\right] \\ &= S_{\tilde{Y}\tilde{Y}}(f) - |H(f)|^2 S_{UU}(f) - |K(f)|^2 S_{UU}(-f) \end{aligned} \tag{10}$$

so that, similar to (6), the definition of EVM for the IQ modulator results

$$\mathrm{EVM} = \sqrt{\frac{\int_{\mathrm{BW}} S_{D_{\tilde{Y}} D_{\tilde{Y}}}(f)df}{\int_{\mathrm{BW}} S_{\tilde{Y}\tilde{Y}}(f)df}}. \tag{11}$$

In principle, the same experimental estimation procedure as the one introduced in Section II-A could be applied to (11). This involves applying to the DUT several independent signal realizations of the input signal U while concurrently recording the output response (see Section III-A for further implications on the identification using a VNA).

In this case, however, it makes sense to define the following matrix:

$$\mathbf{U}(f) = \begin{bmatrix} U_1(f) & U_1(-f)^* \\ \vdots & \vdots \\ U_L(f) & U_L(-f)^* \end{bmatrix} \tag{12}$$

so the two terms of the BLA can be then jointly estimated as

$$\mathbf{H}(f) = \begin{bmatrix} H(f) \\ K(f) \end{bmatrix} = \left(\mathbf{U}^\dagger(f)\mathbf{U}(f)\right)^{-1}\mathbf{U}^\dagger(f)\mathbf{Y}(f). \tag{13}$$

Specific attention must be paid to the conditioning number of $\mathbf{U}^\dagger(f)\mathbf{U}(f)$ to be inverted in (13). While well-conditioning is trivially achieved in the standard SISO case of Section II-A, ill-conditioning might take place here as $U(f)$ and $U(-f)^*$ act as two separate inputs, resembling an MIMO configuration [24] and possibly preventing the correct identification of each BLA contribution. Accounting for the definition in (12), let us write the $\mathbf{U}^\dagger(f)\mathbf{U}(f)$ matrix by making explicit the

term-by-term calculation

$$\mathbf{U}^{\dagger}(f)\mathbf{U}(f) = \begin{bmatrix} \sum_{l=1}^{L} |U_l(f)|^2 & \sum_{l=1}^{L} U_l(f)^* U_l(-f)^* \\ \sum_{l=1}^{L} U_l(f)U_l(-f) & \sum_{l=1}^{L} |U_l(-f)|^2 \end{bmatrix}. \tag{14}$$

Considering the stationarity of the input process, the sums in each term will tend to approximate the expectation operator $\mathbb{E}[\cdot]$ for a sufficiently large number of realizations. In particular, if the previously introduced incorrelation property is assumed, it holds

$$\frac{1}{L}\mathbf{U}^{\dagger}(f)\mathbf{U}(f) \overset{L\to\infty}{\longrightarrow} \begin{bmatrix} \mathbb{E}\left[|U(f)|^2\right] & 0 \\ 0 & \mathbb{E}\left[|U(-f)|^2\right] \end{bmatrix} \tag{15}$$

so that the resulting matrix is diagonal and well-conditioned for $L \to \infty$, whereas a residual correlation might be present in the off-diagonal terms in (14) for any finite value of L, even if the different signal realizations are completely independent of each other [11], [25]. From a practical perspective, this would involve measuring the DUT response to a prohibitively large number of realizations in order to correctly estimate the terms in (8) and, ultimately, the EVM.

To prevent this phenomenon, the L total realizations can be split in B independent groups of P ($P \geq 2$) realizations each, with $L = B \times P$. First, as per the usual procedure, B independent realizations are generated and the corresponding DUT responses are collected. Each of these realizations is then complemented by further P realizations (and corresponding DUT responses) derived from it multiplying by different phase factors. For the bth original realization, the P secondary ones are obtained as follows:

$$U_b(f), \ldots, U_b(f)e^{j\frac{p\pi}{P}}, \ldots, U_b(f)e^{j\frac{(P-1)\pi}{P}}. \tag{16}$$

In this way, the estimates of the PSD, obtained from the complete set of L DUT responses, remain unaffected by the phase terms, while cross correlation terms in (13) sum up exactly to zero as follows:

$$\begin{aligned} \sum_{l=1}^{L} U_l(f)U_l(-f) &= \sum_{b=1}^{B} U_b(f)U_b(-f) \sum_{p=0}^{P-1} e^{j\frac{2\pi p}{P}} \\ &= \sum_{b=1}^{B} U_b(f)U_b(-f)\frac{1-e^{j2\pi}}{1-e^{j\frac{2\pi}{P}}} = 0. \end{aligned} \tag{17}$$

Given this optimal choice of signals, it is possible to estimate all the terms in the proposed BLA decomposition (8) in a well-conditioned way from a fairly small set of measurements, and ultimately measure the EVM for the IQ modulator under test.

III. VNA-Based Implementation

A. Phase-Repeatable Measurements With a VNA

While previously proposed VNA-based EVM characterization methods leverage on time-invariant relative measurements of the input–output signals of the DUT, the presence of a digital interface in the VSG under test prevents from any straightforward signal normalization, hindering the application of the measurement-based model depicted in Section II-B.

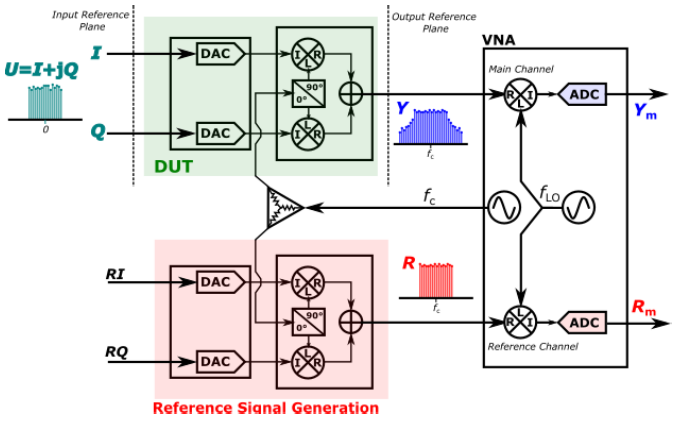

Fig. 3. Block diagram of the proposed measurement setup using a second (unknown) IQ-upconverted signal measured on an additional reference channel. This reference signal can also be flexibly generated by a comb generator or any other suitable method, since it does not embody a traceable waveform standard.

In order to highlight the proposed solution, let us consider the block diagram in Fig. 3. The output Y of the VSG under test at RF frequency f_{RF}, fed by a user-prescribed multitone input complex BB digital signal U, is connected to a first channel (*measurement channel*) of the VNA. Each spectral component of the VSG output signal at frequency f_{RF} is demodulated using a LO at frequency f_{LO} in order to get a component at $f = f_{\mathrm{RF}} - f_{\mathrm{LO}}$ within the IF BW of the VNA. Other spurious and image components can be removed by proper choice of signal period and suitable filtering [26].

For applying the model in Section II-B, the RF output featuring different phase realizations of the multitone excitation must be measured multiple times across the band of interest. Let us consider N noncoherent frequency sweeps. Within the nth sweep, each spectral component is demodulated and digitized in subsequent and independent acquisitions. As a consequence, multiple acquisitions will carry all the time-variant contributions due to acquisition triggering and LO frequency retuning, delivering phase measurements that are not repeatable, thus not usable for VSG characterization.

Thus, let us introduce a second channel (*reference channel*) of the VNA, which shares the same LO and is synchronously triggered with the measurement channel. This reference channel is fed by a reference signal R not *a priori* known and only featuring the following characteristics.

1) R should be kept fixed across the measurements.
2) R must have sufficient power at the frequencies f_{RF} of interest for characterization.

For the nth frequency sweep, the measured components Y_m and R_m at the IF frequency f, on the main and reference channel, respectively, can be modeled as

$$\begin{aligned} Y_m(f,n) &= G_Y(f_{\mathrm{RF}}, f_{\mathrm{LO}})Y(f_{\mathrm{RF}}, n)e^{j2\pi f t(f_{\mathrm{LO}},n)}e^{-j\phi(f_{\mathrm{LO}},n)} \\ R_m(f,n) &= G_R(f_{\mathrm{RF}}, f_{\mathrm{LO}})R(f_{\mathrm{RF}}, n)e^{j2\pi f t(f_{\mathrm{LO}},n)}e^{-j\phi(f_{\mathrm{LO}},n)} \end{aligned} \tag{18}$$

where the subscript m indicates the measurement plane. The terms G_Y and G_R are FRFs representing the systematic LTI cross-frequency effects in the conversion process between the

analog RF/LO signals (at the respective reference planes) and the measured ones at IF. For example, these include the magnitude and phase dispersion of the VNA mixers [27], [28].

The term $e^{j2\pi f t(f_{\mathrm{LO}},n)}$ represents the phase shifts introduced by different triggering time instants $t(f_{\mathrm{LO}}, n)$ of the sweeps. Given that all the receivers in a VNA are triggered synchronously, the same value is assumed at each nth sweep for both the measurement and reference channels. Considering the periodic nature of the signals of interest [29], these terms could be reduced, in principle, to a systematic contribution by using periodic measurement triggering. However, this type of coherent triggering is typically unavailable in standard VNAs, so these terms will be kept in their general form for the following analysis.

The term $e^{-j\phi(f_{\mathrm{LO}},n)}$ expresses the random and unknown contribution to the measurement due to the bin-by-bin retuning of the LO synthesizer across the BW. Indeed, a different LO phase is observed superimposed to components at different frequencies, that is $\phi(f_{\mathrm{LO}}, n) \neq \phi(f'_{\mathrm{LO}}, n)$ if $f_{\mathrm{LO}} \neq f'_{\mathrm{LO}}$. Also, two independent measurements of the component at the same frequency f_{RF} in general involve a different LO phase (albeit the same known frequency f_{LO}), that is $\phi(f_{\mathrm{LO}}, n) \neq \phi(f_{\mathrm{LO}}, n')$ if $n \neq n'$. While it could indeed be possible to use direct digital synthesis to implement some degree of cross-frequency and/or same-frequency phase-coherency of the LO, these functionalities are typically unavailable in classical VNAs, and will not be used here.

Phase-repeatable measurements across different VNA frequency sweeps can be obtained by using data from both measurement and reference channels to remove all the nonsystematic contributions from the acquisition. Considering (18) and a given frequency f at IF, the signals measured during the first acquisition ($n = 0$) result

$$\begin{aligned} Y_m(f,0) &= G_Y(f_{\mathrm{RF}}, f_{\mathrm{LO}})Y(f_{\mathrm{RF}},0)e^{j2\pi f t(f_{\mathrm{LO}},0)}e^{-j\phi(f_{\mathrm{LO}},0)} \\ R_m(f,0) &= G_R(f_{\mathrm{RF}}, f_{\mathrm{LO}})R(f_{\mathrm{RF}},0)e^{j2\pi f t(f_{\mathrm{LO}},0)}e^{-j\phi(f_{\mathrm{LO}},0)}. \end{aligned} \tag{19}$$

By maintaining a fixed yet unknown signal R across the nth measurement sweep, variations in the value R_m measured at the reference channel will map the variations in the LO phase and/or due to the triggering instant among different measurements. At each nth measurement, the following normalized quantity can be computed from the acquired values:

$$\begin{aligned} \overline{Y}_m(f,n) &\stackrel{\mathrm{def}}{=} Y_m(f,n)\frac{R_m(f,0)}{R_m(f,n)} \\ &= G_Y(f_{\mathrm{RF}}, f_{\mathrm{LO}})Y(f_{\mathrm{RF}},n)e^{j2\pi f t(f_{\mathrm{LO}},0)}e^{-j\phi(f_{\mathrm{LO}},0)} \\ &= \overline{G}_Y(f_{\mathrm{RF}}, f_{\mathrm{LO}})Y(f_{\mathrm{RF}},n). \end{aligned} \tag{20}$$

The value of $\overline{Y}_m(f,n)$, linked to the corresponding frequency component $Y(f_{\mathrm{RF}}, n)$ at f_{RF}, is the one that would be measured by the receiver if the LO phase $\phi(f_{\mathrm{LO}}, 0)$ and the triggering instant $t(f_{\mathrm{LO}}, 0)$ were ideally kept the same from the first acquisition ($n = 0$) through the subsequent ones. Such a quantity, independent of n, can be lumped into a generalized systematic LTI transfer function $\overline{G}_Y$ between the measured value $\overline{Y}_m$ and the actual value of interest Y at the RF reference plane of the VSG output. The $\overline{Y}_m$ measurement is also robust with respect to the phase noise in the VNA downconverting LO, as it equally affects both the measurement and reference path, getting factored out in (20).

It is worth stressing that this result is independent of the knowledge of R, allowing to use any suitable reference signal, e.g., the one generated by feeding a generic comb generator device, while not needing any metrology-grade calibration or waveform standard, nor standard traceability [16]. However, the configuration in Fig. 3, in which both the reference and the measured signals share the same upconverting LO at f_{c}, can be considered as the one minimizing unwanted measurement errors as any phase noise present in the common LO signal gets factored out in (20). In all cases, the method is applicable whenever both the measurement and reference signals are precisely synchronized in time and frequency, without any unwanted drifts.

Even though the measurements of $\overline{Y}_m$ are phase-repeatable, no knowledge on the actual phase spectrum, nor any time-domain reconstruction of the signal Y can be achieved from the described acquisitions. Indeed, each frequency component of $\overline{Y}_m$ will embed an unknown yet systematic phase contribution due to the LO. However, this type of cross-frequency information is not needed in order to quantify the EVM, as described hereafter.

B. Measurement-Based EVM Model of a VSG Using a VNA

Let us recall the BLA-based framework for IQ modulators depicted in (8)–(11). The input signal, i.e., the digital signal $U = I + jQ$, is user-imposed and thus exactly known *a priori*. Conversely, the output signal Y, and in particular its BB-equivalent version $\widetilde{Y}$ as in the model in (8), must be retrieved from the measured quantities. By enforcing phase repeatability as from (20) and adapting it to the BB-equivalent formalism, the following relationship holds:

$$\overline{Y}_m(f) = \overline{G}_{\widetilde{Y}}(f)\widetilde{Y}(f) \tag{21}$$

which links the BB-equivalent version $\widetilde{Y}$ of Y to the quantity $\overline{Y}_m$ through the iso-frequency LTI function $\overline{G}_{\widetilde{Y}}$, the latter having the same properties of $\overline{G}_Y$ introduced in (20). Accounting for (8) and (21), the following measurement-based model can be eventually defined [see Fig. 2(d)]:

$$\begin{aligned} \overline{Y}_m(f) &= \overline{G}_{\widetilde{Y}}(f)\widetilde{Y}(f) \\ &= \overline{G}_{\widetilde{Y}}(f)\big[H(f)U(f) + K(f)U(-f)^* + D_{\widetilde{Y}}(f)\big] \\ &= \overline{H}(f)U(f) + \overline{K}(f)U(-f)^* + \overline{D}_{\widetilde{Y}}(f) \end{aligned} \tag{22}$$

where the newly defined terms

$$\overline{H}(f) = \overline{G}_{\widetilde{Y}}(f)H(f); \qquad \overline{K}(f) = \overline{G}_{\widetilde{Y}}(f)K(f) \tag{23}$$

$$\overline{D}_{\widetilde{Y}}(f) = \overline{G}_{\widetilde{Y}}(f)D_{\widetilde{Y}}(f) \tag{24}$$

realize a cascade with the LTI system $\overline{G}_{\widetilde{Y}}$. Indeed, the terms in (23) correspond to new BLA functions, whereas the one in (24) is the new nonlinear stochastic distortion term.

Clearly, the new BLA terms in (23) embed the fixed yet unknown phase offset due to the LO retuning across the BW of interest. Nevertheless, according to (10), the nonlinear stochastic distortion is computed as a deviation from the estimated

magnitude of the BLAs, making the phase of the estimated BLAs irrelevant to the EVM calculation. Hence, despite the fact that the actual phase characteristic of the resulting BLAs will not have any clear physical interpretation, this element will not affect the overall EVM value.

Conversely, phase repeatability across multiple measurements is strictly required. Indeed, if not enforced, each realization at a given frequency used in (4) would embed a different LO phase. This, in turn, would result in the ill-conditioning of the BLA estimation (in both magnitude and phase), as the contributions due to different realizations across different measurements would tend to average out at each bin. It is worth highlighting that this type of behavior fundamentally differs from the previously reported case of a PA as a DUT [7], where the same LO setting is used for measuring both the input and output at a given frequency so that the unknown phase shift due to LO phase contribution automatically cancels out in the numerator of (2).

In (21), on top of the random yet repeatable phase contribution due to the LO, the mapping between the output $\widetilde{Y}$ and the measured $\widetilde{Y}_m$ will also contain a systematic magnitude contribution $|\overline{G}_{\widetilde{Y}}(f)|$, which represents the frequency response of the test-set and downconverting hardware. This term, in principle, could have an influence on both the BLA estimation and the measurement of the output PSD, and should be separately characterized for a subsequent compensation. For example, it was reported in [29] that such a characterization can be achieved by relating the response to the measurements of a rated power meter. However, as long as it does not significantly depend on frequency within the modulation BW, i.e., $|\overline{G}_{\widetilde{Y}}(f)| \approx const$ as expected in properly designed VSGs, it has been shown in [10] that this type of flat-amplitude LTI term does not practically influence the EVM estimation.

IV. Measurement Setup

The measurement setup, shown in Fig. 4, corresponds to the block diagram introduced in Fig. 3. The particular VSG under test including IQ modulation is constituted by the two BB generators of a VSG (Keysight N5182B, with 80-MHz instantaneous BW each) feeding an active analog IQ modulator board (Analog Devices EVAL-ADMV1013).

The reference signal is generated through a similar combination of the two BB generators of a second VSG (Keysight N5182A, with 55-MHz instantaneous BW each) and a passive IQ mixer (Marki Microwave MLIQ1845). Considering that the ADMV1013 modulator performs LO frequency quadrupling internally, an active quadrupler (Marki Microwave AQA2040) is added to the LO path of the MLIQ1845 mixer in the reference channel so to share a common split LO and achieve phase-synchronization between the two channels.

Two internal narrowband receivers of the VNA (N5242B PNA-X by Keysight Technologies), each one featuring a 3-dB IF BW of up to 38 MHz, are used for the measurement and reference channels, respectively. Nevertheless, the proposed EVM measurement technique can be performed with VNA receivers featuring any arbitrarily narrow IF BW by performing bin-by-bin LO sweeps.

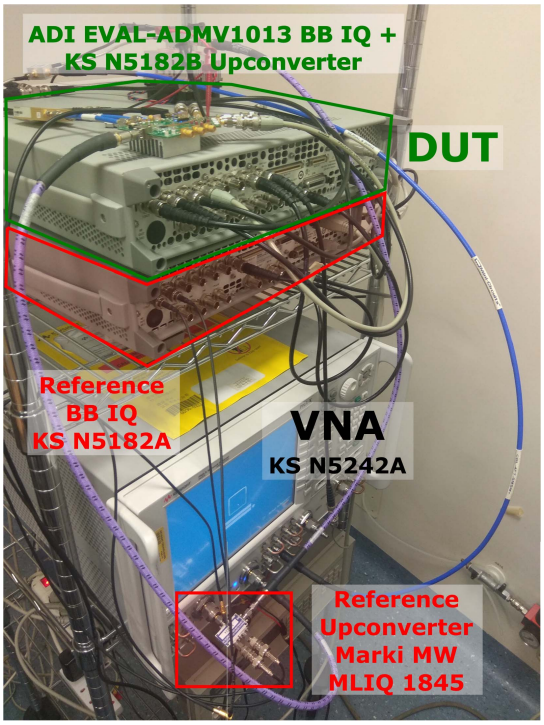

Fig. 4. Photo of the measurement setup used for the experiments, corresponding to the block diagram in Fig. 3.

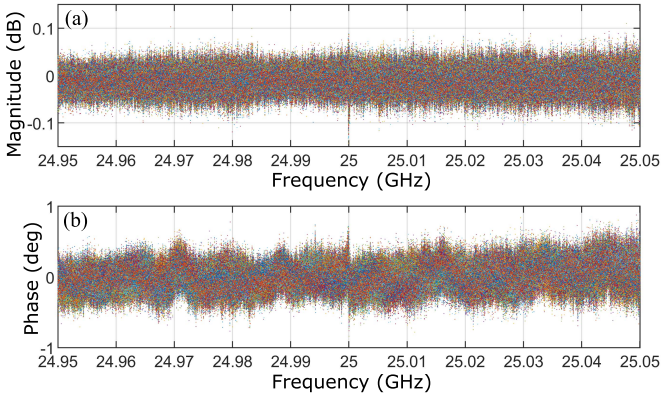

Fig. 5. (a) Magnitude and (b) phase of the ratio $V(f, n)$ across $N = 100$ different VNA sweeps (in different colors).

Given the BB limitations of the reference VSG, the EVM measurement framework is here applicable to modulated signals with up to 100-MHz modulation BW within the frequency range between 24 (lower frequency limit of the analog IQ modulator EVAL-ADMV1013 by Analog Devices) and 26.5 GHz (upper frequency limit of the RF front-end of the VNA in use).

Before all measurements are carried out, the LO feed-through in the DUT channel is precompensated. Without any input signal applied, the dc offset value in the BB IQ modulator is automatically corrected in an iterative fashion until no significant feedthrough component is observed on the output.

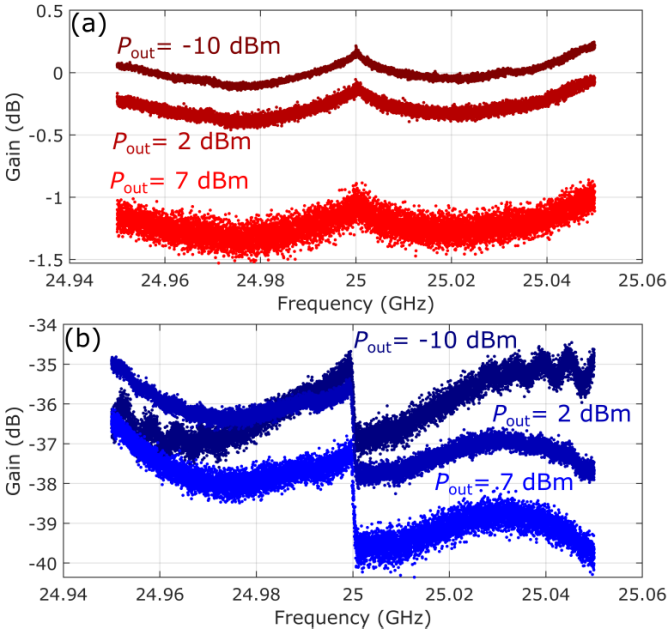

Fig. 6. Magnitude of (a) conversion gain ($\overline{H}$) and (b) IQ imbalance ($\overline{K}$) terms for a 100-MHz-BW random-phase multitone excitation at $f_c = 25$ GHz. Three levels of average output power are reported (average conversion gain magnitude across frequency for $P_{out} = -10$ dBm normalized to 0 dB).

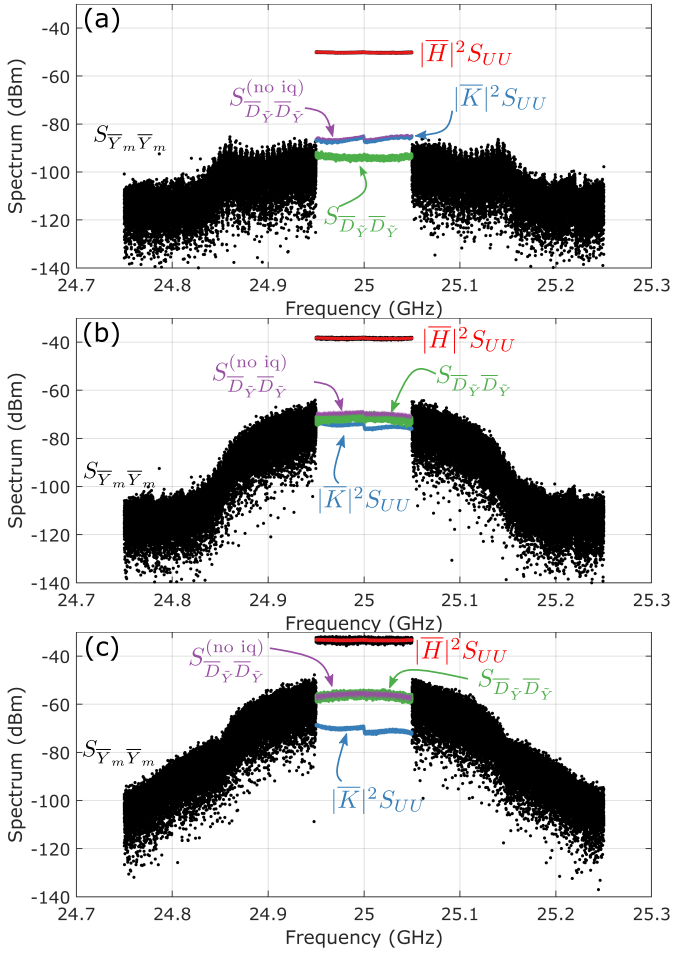

Fig. 7. RF output power spectra of the VSG under test at different RF average powers (a) $P_{out} = -10$ dBm, (b) $P_{out} = 2$ dBm, and (c) $P_{out} = 7$ dBm; highlighting the decomposition of the in-band terms as from the measurement-based EVM model in (22).

V. Experimental Results

A. Phase Repeatability Analysis

As a preliminary step, a phase repeatability analysis of the acquisitions is obtained with the proposed measurement setup. To this aim, both the measurement and reference path are excited by two independent 100-MHz-wide random phase multitone signals with 9 kHz of spacing (for a total of 11 113 tones) around a carrier at $f_c = 25$ GHz, with an average power of -10 dBm each. These signals are kept fixed for $N = 100$ VNA sweeps: that is, $Y(f_{RF}, n)$ and $R(f_{RF}, n)$ do not depend on the sweep index n. Then, using (18), a ratio between quantities at the measurement plane on the two channels can be computed as follows:

$$V(f,n) = \frac{Y_m(f,n)R_m(f,0)}{Y_m(f,0)R_m(f,n)} = \frac{Y(f,n)R(f,0)}{Y(f,0)R(f,n)} = 1. \quad (25)$$

The nominal, sweep-independent equality to 1 is obtained irrespective of the knowledge of the signals on the two channels, as long as they are kept constants and the hypotheses of the VNA measurement model introduced in Section III-A hold. Therefore, the measurement of the ratio $V(f,n)$ across the band of interest repeated over the set of VNA sweeps can be seen as an evaluation of the level of phase-repeatability that can be achieved by using the reference-channel based normalization proposed in this work. The results are reported in Fig. 5. In the test conditions, less than 0.1 dB of magnitude and 1° of phase deviation with respect to unity is observed for all frequencies in the band of interest.

B. EVM Characterization Results

The EVM characterization for the VSG under test was performed using $L = 100$ ($B = 50$, $P = 2$) different phase realizations of a 100-MHz-wide random phase multitone signal with 9 kHz of spacing (for a total of 11 113 tones) around a carrier at $f_c = 25$ GHz. The magnitude of the conversion gain $\overline{H}$ and IQ imbalance $\overline{K}$ terms in (22) are shown in Fig. 6. As from definition, the generic BLA gain components embed all the effects involved in the IQ upconversion process that can be modeled by an LTI system, resulting in the nontrivial interpretation of their frequency behavior. Anyway, there is no need to identify the source of these effects to the extent of the proposed technique. Also, by construction, all values are defined with respect to an arbitrary-amplitude numerical signal U; in Fig. 6, they have been normalized so that the average magnitude of the conversion gain across frequency for $P_{out} = -10$ dBm results 0 dB.

Three different average output power levels are reported, in order to examine the effect of different LSOPs. It can be observed that an increase of the input drive leads to a significant compression of the conversion gain term $\overline{H}$ while keeping the same overall shape across BW. Instead, the IQ imbalance term $\overline{K}$ shows a more complicated dependence on the input power, highlighting the importance of separately modeling and compensating for this contribution.

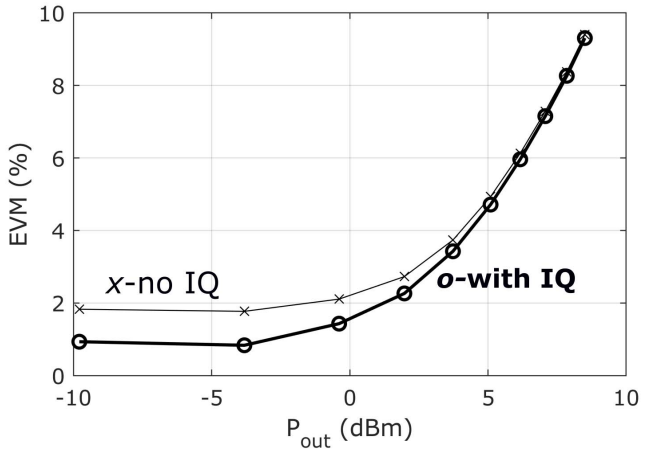

Fig. 8. EVM estimate at $f_c = 25$ GHz (BW $= 100$ MHz) versus RF output power when separating the IQ imbalance term $\overline{K}$ from the distortion as in (10) (circles) compared to the case where IQ imbalance is not separated as in (5), hence included in the EVM calculation (crosses).

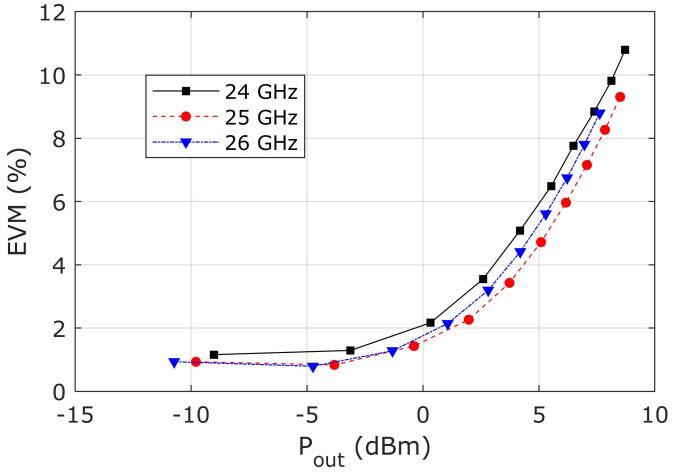

Fig. 9. EVM measurement (IQ imbalance deembedded) versus RF output power at different carrier frequencies (BW = 100 MHz).

Fig. 7 shows the amplitude spectra of the RF output power across a wider BW (including out-of-band regrowth) at the same average power levels as in Fig. 6, depicting the decomposition into linearly correlated terms $|\overline{H}|^2 S_{UU}$ and $|\overline{K}|^2 S_{UU}$ as well as the distortion term $S_{\overline{D}_{\tilde{Y}}\overline{D}_{\tilde{Y}}}$, all resulting from the averaging across the multiple signal realizations. More in detail, Fig. 7 also reports the cases of either accounting or not for the explicit IQ imbalance term in the EVM model in (22). In the former case, the term $\overline{K}$ is identified and suitably separated from the part of the response that is not linearly correlated with the input (green line), leading to a more precise quantification of the contribution uniquely due to nonlinear distortion. In the latter case, the impact of IQ imbalance is instead globally embedded in (and indistinguishable from) the distortion term $S^{(\text{no iq})}_{\overline{D}_{\tilde{Y}}\overline{D}_{\tilde{Y}}}$ (purple line), leading to a substantial overestimation of the nonlinear distortion. At low input power levels and correspondingly low distortion [see Fig. 7(a)], if not identified and suitably deembedded, the impact of IQ imbalance would wrongly be characterized as the main contribution to EVM. Instead, at higher output power, the IQ imbalance term becomes negligible with respect to the uncorrelated nonlinear distortion, which almost totally accounts for the observed EVM value.

This effect can clearly be seen in the power sweep reported in Fig. 8, showing the difference of the EVM profile in the two cases. This example highlights that the proposed method, by exploiting narrowband VNA acquisitions and IQ imbalance deembedding, allows to detect EVM values as low as 1%, which is well suited for 5G FR2 signal specifications. Finally, Fig. 9 reports the EVM (IQ imbalance deembedded) across the power sweep for different carrier frequencies (f_c) covering the usable BW, showing a small yet nonnegligible dependence for the IQ modulator under test.

VI. Conclusion

The demonstrated measurement-based model formulation and corresponding implementation allow to characterize the broadband EVM performance of VSGs in frequency domain using classical VNA instrumentation with narrowband receivers, avoiding time-domain envelope waveform measurement and corresponding absolute phase or waveform calibrations. The technique makes use of periodic excitations statistically compliant to modulated signals of interest for accurately extracting the actual distortion term contributing to the EVM by exploiting a tailored formulation, based on the BLA framework, that separately estimates and deembeds the IQ imbalance effect, thus leading to improved accuracy and sensitivity of the method.

The problem of referring the measurement of the analog output of the VSG to its digital input is solved by using a synchronized reference channel with a stable reference input signal that does not need to be precharacterized or otherwise known. Suitable postprocessing of the acquisitions can remove any time-variant term and yields phase-repeatable measurements carrying a random yet systematic phase contribution due to the LO-based down-conversion in the VNA. This contribution, despite not allowing for time-domain waveform reconstruction, does not impact the EVM characterization as it is removed in the BLA-based linear equalization.

Ultimately, the proposed technique offers an accurate alternative to VSAs, or to equivalent equipment based on broadband receivers extracting the EVM in time domain, which typically require metrology-grade waveform standards and are subject to either limited instantaneous BW or low dynamic range at microwave frequencies.

Appendix

The BB complex envelope $U(f)$ can be split as $I(f) + jQ(f)$, where $I(f)$ and $Q(f)$ are, respectively, the frequency-domain representation of the real-valued input signals in the I and Q branches, respectively. As a consequence, I and Q display Hermitian symmetry, i.e., $I(f) = I(-f)^*$ and $Q(f) = Q(-f)^*$. By computing the correlation between

$U(f)$ and $U(-f)^*$, the following ensues:

$$\begin{aligned}\mathbb{E}[U(f)U(-f)] &= \mathbb{E}[(I(f)+jQ(f))(I(-f)+jQ(-f))] \\ &= \mathbb{E}[I(f)I(-f)-Q(f)Q(-f)] \\ &\quad + j\mathbb{E}[(I(-f)Q(f)+I(f)Q(-f))] \\ &= \mathbb{E}\big[|I(f)|^2-|Q(f)|^2\big] \\ &\quad + j\mathbb{E}\big[(I(f)Q(f)^*+I(f)^*Q(f)\big]. \quad (26)\end{aligned}$$

Therefore, in order to have zero correlation, it is sufficient that the two following conditions hold:

$$\begin{aligned}\mathbb{E}\big[|I(f)|^2\big] &= \mathbb{E}\big[|Q(f)|^2\big] \\ \mathbb{E}\big[I(f)Q(f)^*\big] &= 0. \quad (27)\end{aligned}$$

The first condition states that the signals on the in-phase and quadrature branch of the vector modulator should have the same PSD. Instead, the second imposes that there should not be any correlation between the two branches. Both conditions are satisfied by random-phase multitone signals adopted in this work. More in general, it is sufficient taking the I and Q components of the IQ modulator as two independent realizations of the same stochastic process, like it is typically done for many test signals of interest [7].

ACKNOWLEDGMENT

The authors would like to thank S. Napolitano from Analog Devices, Italy, for providing the modulator board, and Keysight Technologies, USA, for the measurement equipment.

REFERENCES

[1] *Technical Specification 38.101-2, NR; User Equipment (UE) Radio Transmission and Reception; Part 2: Range 2 Standalone*, document, 3GPP. [Online]. Available: https://portal.3gpp.org/desktopmodules/Specifications/SpecificationDetails.aspx?specificationId=3284

[2] K. Remley *et al.*, "Measurement challenges for 5G and beyond: An update from the National Institute of Standards and Technology," *IEEE Microw. Mag.*, vol. 18, no. 5, pp. 41–56, Jul./Aug. 2017.

[3] N. B. De Carvalho and J. C. Pedro, "Large- and small-signal IMD behavior of microwave power amplifiers," *IEEE Trans. Microw. Theory Techn.*, vol. 47, no. 12, pp. 2364–2374, Dec. 1999.

[4] G. L. Heiter, "Characterization of nonlinearities in microwave devices and systems," *IEEE Trans. Microw. Theory Techn.*, vol. MTT-21, no. 12, pp. 797–805, Dec. 1973.

[5] M. D. Mckinley, K. A. Remley, M. Myslinski, J. S. Kenney, and S. B. Nauwelaers, "EVM calculation for broadband modulated signals," in *Proc. ARFTG Microw. Meas. Conf.*, 2004, pp. 45–52.

[6] K. Freiberger, H. Enzinger, and C. Vogel, "A noise power ratio measurement method for accurate estimation of the error vector magnitude," *IEEE Trans. Microw. Theory Techn.*, vol. 65, no. 5, pp. 1632–1645, May 2017.

[7] J. Verspecht, A. Stav, J.-P. Teyssier, and S. Kusano, "Characterizing amplifier modulation distortion using a vector network analyzer," in *Proc. 93rd ARFTG Microw. Meas. Conf. (ARFTG)*, Jun. 2019, pp. 1–4.

[8] Y. Rolain, M. Zyari, E. Van Nechel, and G. Vandersteen, "A measurement-based error-vector-magnitude model to assess non linearity at the system level," in *IEEE MTT-S Int. Microw. Symp. Dig.*, Jun. 2017, pp. 1429–1432.

[9] A. M. Angelotti, G. P. Gibiino, C. Florian, and A. Santarelli, "Broadband error vector magnitude characterization of a GaN power amplifier using a vector network analyzer," in *IEEE MTT-S Int. Microw. Symp. Dig.*, Aug. 2020, pp. 747–750.

[10] G. P. Gibiino, A. M. Angelotti, A. Santarelli, and P. A. Traverso, "Error vector magnitude measurement for power amplifiers under wideband load impedance mismatch: System-level analysis and VNA-based implementation," *Measurement*, vol. 187, Jan. 2022, Art. no. 110254.

[11] T. P. Dobrowiecki, J. Schoukens, and P. Guillaume, "Optimized excitation signals for MIMO frequency response function measurements," *IEEE Trans. Instrum. Meas.*, vol. 55, no. 6, pp. 2072–2079, Dec. 2006.

[12] N. B. Carvalho, K. A. Remley, D. Schreurs, and K. G. Card, "Multisine signals for wireless system test and design [application notes]," *IEEE Microw. Mag.*, vol. 9, no. 3, pp. 122–138, Jun. 2008.

[13] Y. Rolain, W. Van Moer, R. Pintelon, and J. Schoukens, "Experimental characterization of the nonlinear behavior of RF amplifiers," *IEEE Trans. Microw. Theory Techn.*, vol. 54, no. 8, pp. 3209–3218, Aug. 2006.

[14] J. J. De Witt, "Modelling, estimation and compensation of imbalances in quadrature transceivers," Ph.D. dissertation, Dept. Elect. Electron. Eng., Univ. Stellenbosch, Stellenbosch, South Africa, 2011.

[15] J. Verspecht, T. Nielsen, A. Stav, J. Dunsmore, and J.-P. Teyssier, "Modulation distortion analysis for mixers and frequency converters," in *Proc. 95th ARFTG Microw. Meas. Conf. (ARFTG)*, Aug. 2020, pp. 1–4.

[16] Y. Zhang, M. Nie, Z. Zhang, Z. He, and L. Wang, "Repeatable phase spectrum measurements of 75–110-GHz modulated signals using a VNA-based LO phase cancellation technique," *IEEE Trans. Instrum. Meas.*, vol. 70, pp. 1–11, 2021.

[17] Y. Zhang, "Using pulsed-RF signals as phase standards for millimeter-wave modulated measurement and calibration in frequency domain," *IEEE Trans. Microw. Theory Techn.*, vol. 68, no. 7, pp. 2930–2943, Jul. 2020.

[18] Y. Zhang *et al.*, "Precisely synchronized NVNA setup for digitally modulated signal generation and measurement at 5G-oriented millimeter-wave test bands," *IEEE Trans. Microw. Theory Techn.*, vol. 69, no. 1, pp. 833–845, Jan. 2021.

[19] K. A. Remley, P. D. Hale, D. F. Williams, and C.-M. Wang, "A precision millimeter-wave modulated-signal source," in *IEEE MTT-S Int. Microw. Symp. Dig.*, Jun. 2013, pp. 1–3.

[20] K. A. Remley, D. F. Williams, D. Schreurs, and M. Myslinski, "Measurement bandwidth extension using multisine signals: Propagation of error," *IEEE Trans. Microw. Theory Techn.*, vol. 58, no. 2, pp. 458–467, Feb. 2010.

[21] R. Pintelon and J. Schoukens, *System Identification: A Frequency Domain Approach*. Hoboken, NJ, USA: Wiley, 2012.

[22] J. Verspecht, "Generation and measurement of a millimeter-wave phase dispersion reference signal based on a comb generator," in *IEEE MTT-S Int. Microw. Symp. Dig.*, May 2016, pp. 1–4.

[23] Z. Li, Y. Xia, W. Pei, K. Wang, Y. Huang, and D. Mandic, "Noncircular measurement and mitigation of I/Q imbalance for OFDM-based WLAN transmitters," *IEEE Trans. Instrum. Meas.*, vol. 66, no. 3, pp. 383–393, Mar. 2017.

[24] T. P. Dobrowiecki and J. Schoukens, "Linear approximation of weakly nonlinear MIMO systems," *IEEE Trans. Instrum. Meas.*, vol. 56, no. 3, pp. 887–894, Jun. 2007.

[25] T. Dobrowiecki and J. Schoukens, "Measuring a linear approximation to weakly nonlinear MIMO systems," *Automatica*, vol. 43, no. 10, pp. 1737–1751, Oct. 2007.

[26] J. Verspecht, J.-P. Teyssier, and T. S. Nielsen, "Method and system of preventing interference caused by images," U.S. Patent 10 003 419, Jun. 19, 2018.

[27] J. Verspecht and K. F. Anderson, "Method and system for characterizing phase dispersion in intermediate frequency channel of receiver," U.S. Patent 9 520 954, Dec. 13, 2016.

[28] K. F. Anderson, J. Verspecht, and T. S. Nielsen, "Method and apparatus for characterizing local oscillator path dispersion," U.S. Patent 9 793 857, Oct. 17, 2017.

[29] A. M. Angelotti, G. P. Gibiino, T. Nielsen, F. F. Tafuri, and A. Santarelli, "Three port non-linear characterization of power amplifiers under modulated excitations using a vector network analyzer platform," in *IEEE MTT-S Int. Microw. Symp. Dig.*, Jun. 2018, pp. 1021–1024.

Alberto Maria Angelotti (Member, IEEE) received the Ph.D. degree in electronics, telecommunications, and information technology engineering from the University of Bologna, Bologna, Italy, in 2021.

Since 2017, he has been with the Department of Electrical, Electronic, and Information Engineering "Guglielmo Marconi," University of Bologna, where he is currently a Post-Doctoral Research Fellow. His research interests include microwave instrumentation, nonlinear measurements, and characterization of gallium nitride devices, and power amplifiers.

Gian Piero Gibiino (Member, IEEE) received the dual Ph.D. degree from the University of Bologna, Bologna, Italy, and KU Leuven, Leuven, Belgium, in 2016.

He is currently a Research Associate with the Department of Electrical, Electronic, and Information Engineering "Guglielmo Marconi," University of Bologna. His research interests include RF/microwave instrumentation and measurement, as well as measurement-based behavioral modeling and performance enhancement of RF/microwave devices and circuits.

Dr. Gibiino is a member of the IEEE Microwave Theory and Techniques (MTT) and IEEE Instrumentation and Measurement (I&M) Societies, the Automatic Radio Frequency Techniques Group (ARFTG), the European Microwave Association (EuMA), and the Italian Association of Electrical and Electronic Measurements (GMEE). He is also an Affiliate Member of MTT TC-2 (design automation) and TC-3 (microwave measurements).

Alberto Santarelli (Member, IEEE) received the Laurea degree *(cum laude)* in electronic engineering and the Ph.D. degree in electronics and computer science from the University of Bologna, Bologna, Italy, in 1991 and 1996, respectively.

From 1996 to 2001, he was a Research Assistant with the Research Centre for Computer Science and Communication Systems, Italian National Research Council (IEIIT-CNR), Bologna. In 2001, he joined the Department of Electrical, Electronic, and Information Engineering "Guglielmo Marconi" (DEI), University of Bologna, where he is currently an Associate Professor and during his academic career, he has been a Lecturer of high-frequency electronic circuits, applied electronics, and power electronics. His main research interests include nonlinear characterization and modeling of electron devices and nonlinear circuit design.

Dr. Santarelli is a member of the European Microwave Association (EuMA).

Pier Andrea Traverso (Member, IEEE) was born in Modena, Italy, in 1969. He received the M.S. degree (Hons.) in electronic engineering and the Ph.D. degree in electronic and computer science engineering from the University of Bologna, Bologna, Italy, in 1996 and 2000, respectively.

From 2000 to 2002, he received a research grant from the Italian National Research Council (CSITE-CNR Institute), Bologna, for his research activity concerning microwave electron device characterization and nonlinear empirical modeling. Since 2002, he has been with the Department of Electrical, Electronic and Information Engineering "Guglielmo Marconi," University of Bologna, where he is currently an Associate Professor of electronic measurement. He has coauthored more than 120 international journal/conference technical papers. His main research interests include nonlinear dynamic system characterization and empirical modeling, microwave and millimeter-wave semiconductor device characterization and modeling, smart sensor nodes, and advanced sampling instrumentation and techniques.

Dr. Traverso is a member of the Italian Association of Electrical and Electronic Measurement (GMEE) and the IEEE TC-10, Committee on Waveform Generation, Measurement, and Analysis.